Appl. Phys. B 71, 457–465 (2000) / Digital Object Identifier (DOI) 10.1007/s003400000351

Applied Physics B
Lasers
and Optics

Generation of 10 to 50 fs pulses tunable through all of the visible and the NIR

E. Riedle, M. Beutter, S. Lochbrunner, J. Piel, S. Schenkl*, S. Spörlein, W. Zinth

Sektion Physik, Ludwig-Maximilians-Universität München, Oettingenstrasse 67, 80538 München, Germany
(Fax: +49-89/2178-2902, E-mail: eberhard.riedle@physik.uni-muenchen.de)

Received: 29 November 1999/Published online: 5 July 2000 –

Abstract. Noncollinearly phase-matched optical parametric amplifiers (NOPAs) pumped by the blue light of a frequency-doubled Ti:sapphire regenerative amplifier are a convenient source of continuously tunable ultrashort pulses in the visible and near infrared for spectroscopic experiments. We present the underlying principles, report recent improvements and describe the experiences gained from the routine use of a number of NOPAs in our laboratories. We find that the setup can easily be optimized for the given experimental requirements. Typical output-pulse energies in the visible are 5 to 10 μJ and a few μJ in the NIR from 200 μJ regenerative-amplifier pulses at 800 nm. From 460 to 700 nm, pulse lengths between 10 and 20 fs are routinely achieved, while the length increases monotonically from about 20 fs at 900 nm to just below 50 fs at 1600 nm. In all cases this corresponds to a dramatic shortening compared to the length of the pump pulses of around 100 fs. First results show that the 700 to 900 nm region can be accessed with sub-50-fs pulse lengths by use of an intermediate white-light generator in a two-stage setup.

PACS: 42.65.Yj; 42.65.Re; 42.79.Nv

Many processes of physical, chemical or biological interest proceed on an ultrafast time scale, sometimes with a decay time of just a few tens of femtoseconds or even strongly non-exponential dynamics. The best possible direct investigation of such rapid processes is in pump–probe experiments, i.e. the sample of interest is disturbed with a first light pulse and subsequently the evolving state of the system is probed with a second pulse. In such an experiment the temporal resolution achieved is limited by the length of the light pulses and extremely short pulses are needed.

Femtosecond pulses were first generated with the CPM laser at a fixed wavelength of about 620 nm and moderate pulse energies [1]. To boost the energies dye amplifiers at low repetition rate were used [2]. Tunability was gained by continuum generation and a second stage of amplification in a suitable dye [3]. Finally, pulse shortening to sub-10-fs length was reached by spectral broadening in a single-mode fiber and compression in a combination of prisms and gratings [4]. Such laser systems were quite successful tools for spectroscopic experiments; however, their operation is quite demanding.

A largely improved reliability and increased ease of handling is available with laser systems based on mode-locked Ti:sapphire lasers. The weak, high-repetition-rate output of the primary oscillator can be well amplified in chirped-pulse regenerative amplifiers (RGAs) [5] yielding typically an output around 1 mJ at 1 kHz and 100 fs duration. The wavelength of the pulses is only slightly tunable in the vicinity of 800 nm. For most spectroscopic experiments one does need, however, pulses at differing wavelengths dictated by the absorption features of the sample.

A convenient method to derive fully tunable pulses from a RGA is optical parametric conversion. If the fundamental output of the RGA is used as pump, NIR pulses can be generated with high efficiency and pulse lengths down to below 50 fs [6, 7]. Visible and UV pulses can then be derived by frequency conversion in nonlinear optical crystals [8–11]. Alternatively the RGA output can first be frequency-doubled and a blue-pumped optical parametric amplifier (OPA) can then be used for the direct generation of visible pulses. If a combination of optical parametric generation (OPG) and amplification is used, fairly long pulses result [12–16]. A large improvement in performance is reached by continuum seeding of the OPA [17, 18]. The group-velocity mismatch between the three interacting waves does limit the obtainable pulse lengths to above 50 fs if the classical collinear phase-matching geometry is used.

Gale and coworkers demonstrated in a synchronously pumped optical parametric oscillator (OPO) that this limitation can be avoided in a noncollinear geometry [19–21]. In earlier work we were able to show that this concept can successfully be used in kHz systems and furnishes fully tunable sub-20-fs pulses at visible wavelengths [22, 23]. Much work based on this concept has been reported in the past two years. De Silvestri and coworkers demonstrated that the minimization of the chirp of the continuum leads to even

*_Present address_: Université de Lausanne, Bâtiment de Physique IPMC, CH-1015 Lausanne, Switzerland

shorter pulses [24, 25]. They also showed that these pulses with a small chirp can be compressed by chirped mirrors instead of a prism sequence [26]. Kobayashi and coworkers showed that by tilting the pump-pulse front [27, 28] the pulses can be shortened to 4.7 fs [29]. In our own work we were able to broaden the understanding of the operational characteristics [30, 31] and extend the tuning range of the blue-pumped NOPA out to 1600 nm [32].

The NOPA scheme has now matured to the point where spectroscopic experiments with tunable sub-20-fs pulses are possible. In our own laboratories a number of different pump laser/NOPA combinations are successfully used and we want to report on the experiences gained. We first summarize the underlying principles and discuss the influence of the pump-pulse group velocity. Next we present an overview of the performance in the three tuning ranges to be considered and finally give examples of the resulting two-color spectrometers.

1 Noncollinear phase matching for broadband optical parametric amplification

In an OPA photons contained in a short-wavelength pump beam are split into one signal and one idler photon at longer wavelengths. In this paper we discuss the situation with blue pump, visible signal and NIR idler photons. The "active" medium is a nonlinear optical crystal, such as β-barium borate (BBO). For efficient conversion the phase velocities of pump, signal and idler are matched by proper orientation of the birefringent crystal. This results in the well-known phase-matching condition for the wave vectors $\boldsymbol{k}_1, \boldsymbol{k}_2$ and $\boldsymbol{k}_\mathrm{p}$ of signal, idler and pump (see Fig. 1c)

$$\Delta\boldsymbol{k} = \boldsymbol{k}_\mathrm{p} - \boldsymbol{k}_1 - \boldsymbol{k}_2 = 0 \tag{1}$$

Unfortunately, however, phase matching does not simultaneously assure matching of the three group velocities. Therefore the three pulses propagate at differing speeds in the crystal. As a result for blue-pump pulses the amplified signal and idler pulses exiting the crystal are typically 100 fs long for collinear phase matching in a 1 or 2 mm BBO crystal.

The situation is illustrated in Fig. 1a. A very short visible seed pulse (signal; open box) is injected into the crystal and some idler (hashed box) is generated. The idler pulse propagates somewhat faster than the signal ($\upsilon_{\mathrm{g},2} > \upsilon_{\mathrm{g},1}$). Continuously the signal and idler pulses are amplified as they travel through the crystal. In addition the signal generates more idler just as the idler generates more signal. Due to the differing group velocities, these new signal photons are added onto the leading edge of the signal pulse and the new idler photons due to the signal pulse are added onto the trailing edge of the idler pulse. As a result lengthened pulses cannot be avoided in collinear phase-matched visible OPAs.

Work by Gale and coworkers [19–21] demonstrated an elegant solution to the problem of pulse lengthening in collinearly phase-matched parametric interaction. They used a noncollinear arrangement in a quasi-CW-pumped visible OPO to produce sub-20-fs pulses. The aim of this geometry is to obtain very broad amplification bandwidth by broadband phase matching and consequently the necessary spectral width to support an extremely short pulse. As will be shown, this simultaneously ensures matching of the group velocities.

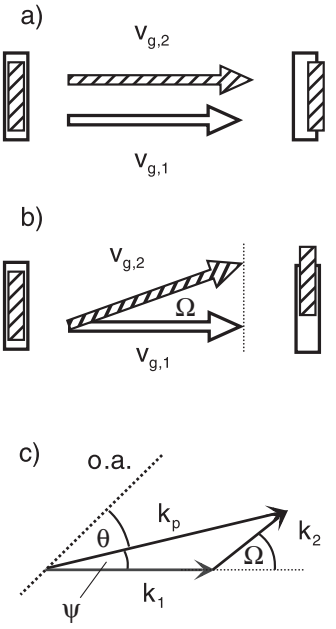

Fig. 1. a The larger group velocity $\upsilon_{\mathrm{g},2}$ of the idler wave within the nonlinear crystal leads to a separation of the idler pulse (*hashed*) and the signal pulse propagating with group velocity $\upsilon_{\mathrm{g},1}$. Since signal and idler are continuously regenerated from each other, considerable lengthening results in a collinear geometry. **b** With a suitable angle between the signal and idler, effective group-velocity matching can be reached in the propagation direction of the signal wave. As a result extremely short visible pulses can be generated in NOPAs. **c** Definition of various quantities used in the discussion of noncollinear phase matching

Broadband phase matching requires that the wave vector mismatch $\Delta\boldsymbol{k}$ does not change with a change of the seed-pulse wavelength. If $\Delta\boldsymbol{k}$ is expanded in powers of the seed wavelength detuning $\Delta\lambda_1$ for constant pump wavelength λ_p

$$\Delta\boldsymbol{k} = \Delta\boldsymbol{k}_0 + \frac{\partial\Delta\boldsymbol{k}}{\partial\lambda_1}\Delta\lambda_1 + \frac{1}{2}\frac{\partial^2\Delta\boldsymbol{k}}{\partial\lambda_1^2}\Delta\lambda_1^2 + \ldots \tag{2}$$

broadband phase matching requires

$$\frac{\partial\Delta\boldsymbol{k}}{\partial\lambda_1} = 0 \tag{3}$$

besides the usual phase-matching condition $\Delta\boldsymbol{k}_0$. This condition can easily be related to the group velocities. First we use the energy conservation in the parametric interaction (λ_i being vacuum wavelengths)

$$\frac{1}{\lambda_\mathrm{p}} = \frac{1}{\lambda_1} + \frac{1}{\lambda_2} \tag{4}$$

to derive the following auxiliary relations valid within the crystal

$$\frac{\partial\lambda_2}{\partial\lambda_1} = -\frac{\lambda_2^2}{\lambda_1^2} \tag{5}$$

$$\frac{\partial k_1}{\partial\lambda_1} = \frac{\partial}{\partial\lambda_1}\frac{2\pi n_1}{\lambda_1} = 2\pi\frac{\lambda_1\dfrac{\partial n_1}{\partial\lambda_1}n_1}{\lambda_1^2} = -\frac{2\pi c}{\lambda_1^2\upsilon_{\mathrm{g},1}} \tag{6}$$

$$\frac{\partial k_2}{\partial\lambda_1} = \frac{\partial}{\partial\lambda_2}k_2\frac{\partial\lambda_2}{\partial\lambda_1} = \left(-\frac{2\pi c}{\lambda_2^2\upsilon_{\mathrm{g},2}}\right)\left(-\frac{\lambda_2^2}{\lambda_1^2}\right) = \frac{2\pi c}{\lambda_1^2\upsilon_{\mathrm{g},2}}\,. \tag{7}$$

According to the scheme shown in Fig. 1c the vectorial phase mismatch can be decomposed into the components parallel and perpendicular to $\boldsymbol{k}_1$

$$\Delta k_{\parallel} = k_1 + k_2 \cos\Omega - k_\mathrm{p} \cos\Psi \tag{8}$$

$$\Delta k_{\perp} = k_2 \sin\Omega - k_\mathrm{p} \sin\Psi \,. \tag{9}$$

Differentiation leads to

$$\frac{\partial \Delta k_{\parallel}}{\partial \lambda_1} = \frac{\partial k_1}{\partial \lambda_1} + \frac{\partial k_2}{\partial \lambda_1} \cos\Omega - k_2 \sin\Omega \frac{\partial \Omega}{\partial \lambda_1} \tag{10}$$

$$\frac{\partial \Delta k_{\perp}}{\partial \lambda_1} = \frac{\partial k_2}{\partial \lambda_1} \sin\Omega + k_2 \cos\Omega \frac{\partial \Omega}{\partial \lambda_1} \tag{11}$$

as both the angle Ψ and λ_p are assumed to be constant. According to the assumption of broadband phase matching, i.e. equation (3), both components of $\frac{\partial \Delta \boldsymbol{k}}{\partial \lambda_1}$ must vanish. Multiplication of equation (10) with $\cos\Omega$ and equation (11) with $\sin\Omega$ and subsequent addition then yields

$$\frac{\partial k_1}{\partial \lambda_1} \cos\Omega + \frac{\partial k_2}{\partial \lambda_1} = 0 \tag{12}$$

Together with equations (6) and (7) this is equivalent to

$$\upsilon_{\mathrm{g},2} \cos(\Omega) = \upsilon_{\mathrm{g},1} \,. \tag{13}$$

This means that a vanishing value of $\frac{\partial \Delta \boldsymbol{k}}{\partial \lambda_1}$ equivalent to the fact that the projection of the idler group velocity onto the signal wave vector is equal to the signal group velocity.

For type I phase-matched BBO and 400 nm pump light the idler ($\lambda > 800$ nm) group velocity is always larger than the signal ($\lambda < 800$ nm) group velocity and a suitable angle $\Omega(\lambda_\mathrm{signal})$ can be found. The pump seed angle Ψ, which can be chosen experimentally, is related to Ω according to

$$\Psi(\lambda_\mathrm{signal}) \approx \frac{\Omega(\lambda_\mathrm{signal})}{\left(1 + \frac{\lambda_\mathrm{idler}}{\lambda_\mathrm{signal}}\right)} \,. \tag{14}$$

The derivation of this approximate relationship (less than 4% error) relies on the fact that the refractive indices of the o-polarized signal and idler are nearly equal and in turn equal to the effective refractive index of the e-polarized pump. For the 500 to 700 nm region Ψ only varies slightly between 3° and 4° [22]. All angles are considered inside the BBO crystal.

The noncollinear situation is illustrated in Fig. 1b. Now the extra signal photons generated by the amplification of the idler are produced at the same "horizontal" position as the ones due to amplification of the signal itself, and no lengthening of the pulse results. The transversal displacement of the idler only leads to a slight spatial widening of the signal beam.

A broader picture of the phase-matching situation is obtained if the phase mismatch is calculated for a variation of wavelengths and any geometry of interest. Such calculations have been shown by different authors [27, 30, 31] and the proper choice of angles is found to be well predicted by equations (13) and (14). A detailed numerical simulation was also reported recently [33]. For calculations of the phase-matching angles in the noncollinear parametric interaction the program SNLO written by Smith [34] is most helpful. It can be downloaded from http://www.sandia.gov/imrl/XWEB1128/Xframe.htm. Any angles and geometries needed for the alignment of a NOPA can easily be calculated with the help of this program.

In the original OPO reported by Gale et al. [20] the tuning range was limited by the resonator optics and the operation of the OPO depends critically on a very high average pump power. Wilhelm et al. were the first to show that a traveling wave noncollinearly phase-matched OPA pumped by blue pulses at 1 kHz repetition rate can readily yield sub-20-fs pulses tunable throughout the visible [22, 23].

2 Influence of the continuum chirp and the pump group velocity

The principal parts of a NOPA are shown schematically in Fig. 2. Following earlier work by Reed et al. [17, 18, 35] a high-quality single-filament continuum is generated by focusing a small fraction of the 800 nm RGA output tightly into a 3 mm sapphire plate. The resulting spectral distribution can be seen in Fig. 3. It consists of a flat plateau between 470 and 720 nm, while a highly structured spectrum is found around the pump wavelength, i.e. between 750 and 870 nm. Recently it was argued that the flat plateau in the visible is due to multiphoton excitation of electrons to the conduction band and spectral superbroadening caused by the free electrons [36]. The highly structured region around 800 nm seems to be due to more conventional self-phase modulation. The chirp of the

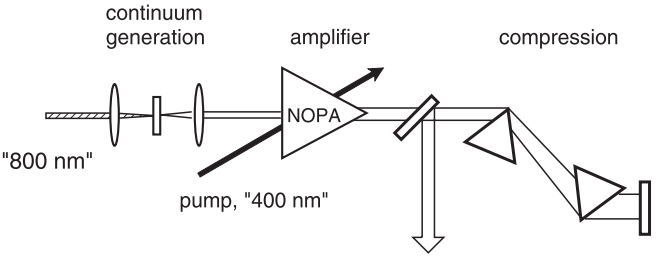

Fig. 2. Schematic of a single-stage NOPA consisting of a "800 nm" pumped continuum generator, the "400 nm" pumped amplifier in noncollinear geometry and the prism compressor

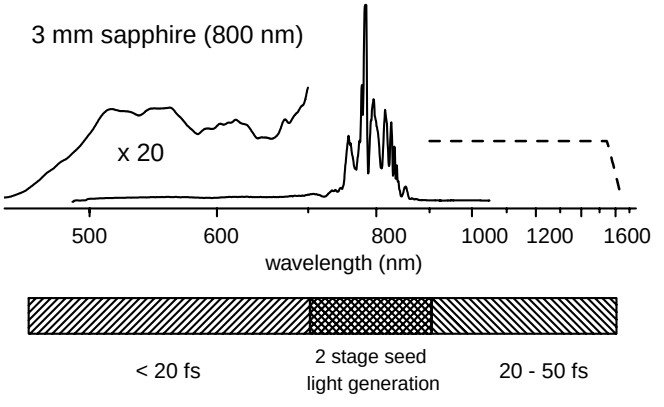

Fig. 3. Overview of the tuning range and output pulse length of a blue-pumped NOPA. The principal range is determined by the spectral distribution of the continuum generated in a sapphire disk. Around the pump wavelength the continuum is highly structured and a two-stage setup has to be used

continuum is moderate throughout the plateau [24, 29] and limited spectral regions can be well compressed [30].

In the NOPA a type I phase-matched BBO crystal of 1 or 2 mm length and cut at a typical angle of 32° is used as the nonlinear medium in a nonplanar geometry [22]. The broad amplification bandwidth of the noncollinear setup does allow the generation of strong pulses with a wide enough spectral bandwidth to support extremely short pulse lengths. The resulting pulses are chirped as they leave the BBO crystal and have to be compressed. A simple two-prism compressor (fused silica) is sufficient for sub-20-fs pulses [22]. Even shorter pulses can be obtained from seed light with less chirp [24, 25]. The adverse influence of the tilted pump-pulse front can be overcome by proper optical arrangements [27–29]. While these improvements lead to reduced pulse lengths, they make the system less easily tunable and intrinsically lead to extremely broad pulse spectra. Both aspects might seriously limit the usefulness of the setup for spectroscopic applications requiring Fourier- transform-limited pulses. The broad spectra might, however, be well suited for investigations utilizing multichannel detection.

It should be emphasized that the advantage of noncollinear phase matching for the generation of ultrashort light pulses can only be utilized if an OPA is seeded with compressible continuum light. If an OPG is used instead of a white-light generator, the differing group velocities of the signal and idler pulses and in particular the pump pulses will lead to incompressible pulse lengthening. In the NIR, i.e. when the OPA is pumped by 800 nm pulses, the differences in group velocities are quite small and pulses as short as 14.5 fs have been generated with suitably short pump pulses in collinear setups [37–39]. Earlier attempts to generate visible sub-100-fs pulses with tilted-pulse geometries were limited by the fact that simultaneous matching of all three group velocities is not possible [15, 16, 40].

Once the necessary amplification bandwidth is secured by the proper geometry, the output characteristics of the NOPA are mainly determined by the interplay of the continuum chirp, the length of the pump pulse and the group velocity of the pump, i.e. the signal/pump and idler/pump group-velocity mismatch (GVM). Unlike the situation encountered in traditional optical amplifiers like dye solutions or Ti:sapphire with nanosecond or even microsecond storage time, in an OPA amplification can only happen if the pump and seed light overlap both in space and time. For a chirped-seed continuum the blue and green spectral components are delayed relative to the red ones by a few 100 fs. Desired components can only be amplified when they arrive at the nonlinear crystal simultaneously with part of the pump pulse. If the pump pulse is extremely short, the bandwidth for a given chirp will be small and a very weakly chirped seed light is needed for the generation of ultrashort pulses. For moderately short pump pulses the chirp can be much larger. We were indeed able to show that the variation of the seed chirp and appropriate compression after the NOPA can be used to vary the output-pulse length [22].

The signal/pump GVM is on the order of 100 fs/mm in type I BBO and leads to a relaxation of the need for temporal overlap in a NOPA. The e-polarized blue pump is slower than the o-polarized visible signal and therefore the pump will amplify differing temporal fractions of the seed light as it propagates through the crystal. For the positively chirped seed pulse, longer-wavelength components are amplified at the beginning of the crystal while shorter wavelength components are amplified at the end; this leads to a broader output spectrum. We have indeed found nearly twice the spectral bandwidth with a 4 mm crystal as compared to a 2 mm one. If this slippage is used to compensate for chirp on the continuum-seed light, a non-Gaussian spectrum results. On the other hand a moderate chirp and a moderately short pump pulse of 130 fs duration have been found to produce nearly Gaussian spectra [31].

The situation can be well described in terms of chirped-pulse amplification (CPA). A lack of chirp leads to very high intensities for a given pulse energy. Consequently saturation, back-conversion and even self-phase modulation will start at moderate output energies, far below the level attainable in more conventional visible OPAs [41]. An increased chirp – into the nanosecond regime – has been suggested as a possibility for large pump- and output-pulse energies [42]. This proposition has not yet been tested for ultrashort pulses; however for picosecond pump pulses it has already been demonstrated [43].

3 Operation in the visible (450–700 nm)

NOPAs were set up in our laboratories in various configurations and with a variety of pump lasers. Initially we used a home-built 1 kHz RGA with a center wavelength of 810 nm and a 70 fs pulse length (system 1). Further experiments were performed with a Clark MXR CPA 2001 delivering 130 fs pulses at 775 nm and 1 kHz repetition rate (system 2) and some experiments used a 20 Hz system at 860 nm and a pulse duration of about 110 fs (system 3). We find all of them well suited to pump a NOPA and only the pulse-to-pulse fluctuations and the spatial profile are of real concern.

The plateau region of the seed continuum (see Fig. 2) and the IR cutoff of BBO around 2.7 μm, that eventually leads to absorption of the idler, determine the tuning range of 460 to 700 nm typically realized. Tuning is mainly achieved by a change in the delay between the pump and the chirped seed, i.e. by selection of the desired portion of the spectrum. The seed/pump angle and the tilt of the BBO crystal have to be changed only slightly. We routinely compress these pulses to lengths below 20 fs. Output energies as high as 11 μJ in a single-stage NOPA and 15 μJ in a two- stage NOPA have been obtained. As a rule of thumb the quantum efficiency is 15% from blue pump light to tunable visible output. Typically about 200 μJ RGA output is frequency-doubled in a thin BBO crystal to furnish 60 μJ blue-pump pulses.

The high efficiency in a single amplification stage is due to two facts. 1) In the small-signal limit the parametric conversion depends on the product of signal and idler amplitudes. As the two waves are effectively group-velocity matched, there is no temporal walk-off even for the fairly long crystals used. 2) The geometric walk-off of the e-polarized pump beam is very close to the pump/seed angle used and this leads to collinear energy transport despite the noncollinear phase matching [20–22].

The pulse-to-pulse fluctuations can be kept as small as 1% RMS with a low-noise RGA [31]. This is possible because the highly nonlinear continuum generation does not enter into the fluctuations. The nearly perfect temporal overlap of signal

and idler pulses leads to an extremely large single-pass amplification factor – values as high as 10^8 have been reported [44]. With respect to the seed the NOPA is operated in saturation and the high conversion efficiency leads to pump-power limiting of the output, i.e. the output fluctuations are nearly equal to the fluctuations of the blue pump pulses.

The visible pulses can be well compressed in prism compressors. Down to below 30 fs SF10 prisms are sufficient and easy to handle. The spacing depends on the amount of material used in the NOPA and the material between the NOPA and the spectroscopic experiment that has to be precompensated. A typical value for SF10 is 15 cm at 500 nm and 40 cm at 700 nm. For even shorter pulses fused-silica prisms have been used successfully, with a typical spacing of 70 and 150 cm, respectively. For sub-10-fs pulses prism–grating compressors [28] or chirped mirrors [26] were used by others. Recently it was demonstrated that the compression can be automated if a pulse shaper based on a liquid-crystal mask is used [45].

In Fig. 4a the spectrum of 630 nm pulses is shown when a low chirp seed is amplified in a 2 mm BBO. Due to the effects discussed above the spectrum is flat-top-shaped. This leads to the result that for a particular setting of the compressor fairly smooth-looking pulses of 12 fs duration (sech^2 shape) can be obtained (see Fig. 4b). With further optimization of the compressor a duration of 9.7 fs is achieved; however some wings have developed under these conditions. Fourier transformation of the spectrum under the assumption of constant spectral phase indeed predicts these wings. We therefore believe that longer pump pulses and the resulting smoother spectra are preferable in spectroscopic applications. Investigations are under way to check the possibility of chirping the pump pulses derived from sub-50-fs RGAs in order to obtain improved-quality NOPA pulses.

With mJ RGA pulses readily available the question of energy scaling is often raised. We usually focus the pump pulse

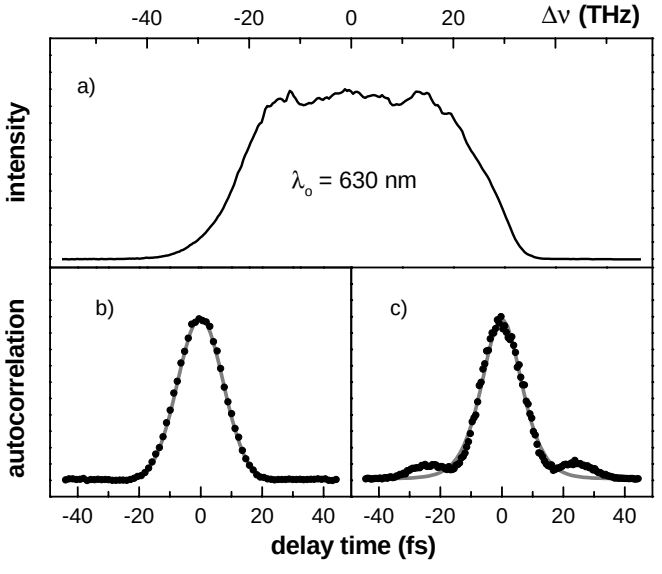

Fig. 4. a Spectrum of a NOPA pulse at 630 nm central wavelength. **b** This pulse can be compressed to 12 fs duration (sech^2 shape) in a fused-silica prism compressor. **c** For a different alignment of the compressor the pulse length is decreased to 9.7 fs. Under these conditions wings show up in the pulse corresponding to the flat-top spectrum

in front of the OPA crystal and adjust the pump intensity by translation of the crystal to typically a value of 50 GW/cm^2. In this way pump energies as low as 7 μJ were sufficient for stable operation [22]. Pump pulses above 80 μJ tend to lead to an air breakdown and are therefore not acceptable in the present geometry. If this constraint were removed, the question of the tilted pump-pulse front (relative to the signal pulse) will gain in importance. For increased pump energy a larger pump spot will have to be used and the tilt will lead to amplification of different wavelength segments in the opposing sides of the interaction region. This lateral chirp can indeed be observed, but it is not yet a significant effect. Kobayashi and coworkers have shown that the pump-pulse front can be properly tilted through the use of a combination of prism and telescope to avoid this problem [28, 29]. The resulting setup couples the pulse tilt and the intensity and is therefore not easily aligned. The above-mentioned idea of chirped-pulse amplification might be a better approach.

4 Operation in the near infrared (900–1600 nm)

The success of the blue-pumped NOPA in the generation of extremely short tunable visible pulses depends on the fact that the noncollinear geometry allows for effective group-velocity matching between signal and idler pulses (see Sect. 2). This is in turn due to the dispersion properties of BBO, i.e. that the idler group velocity is larger than the signal one. If short tunable NIR pulses are needed in a spectroscopic experiment, the straightforward approach will be to pump an OPA with the RGA fundamental output. However, a 800-nm-pumped OPA with type I or II phase-matched BBO can only generate pulses down to wavelengths as short as 1100 nm, and the operation of a system with all three pulses (pump, signal and idler) in the infrared is technically and operationally challenging. Usage of the idler from a blue-pumped NOPA is possible and indeed 9 fs NIR pulses were reported [28]. This does, however, require very complicated optics to correct for the transversal chirp and pulse-front tilt. Alternatively we have investigated the question of how well a blue-pumped NOPA is suited for the generation of NIR pulses [32] if the NOPA is directly seeded with the NIR portion of the continuum.

A simple phase-matching calculation shows that the amplification bandwidth expected for a 1 mm BBO crystal should be sufficient to produce 20 fs pulses around 900 nm and even at 1600 nm 50 fs should be reachable [32]. The calculated bandwidth is highest for the collinear geometry but a slight angle between pump and seed light does not dramatically change the situation. Preliminary experiments did indeed confirm these expectations; however the output pulse energies were quite low. This is due to the temporal walk-off between signal and pump and the resulting reduced parametric gain.

We therefore set up a two-stage NOPA as shown schematically in Fig. 5 [32]. BBO crystals of 1 or 2 mm length were used in both the preamplifier and the booster amplifier. 20% of the blue-pump light was used for the preamplifier. We initially tested the setup in the visible and found it quite easy to operate, as the near-perfect alignment needed to reach high conversion efficiency in a single-stage NOPA is not necessary any more. Pulse energies as high as 15 μJ around 500 nm were obtained with an excellent transversal mode quality.

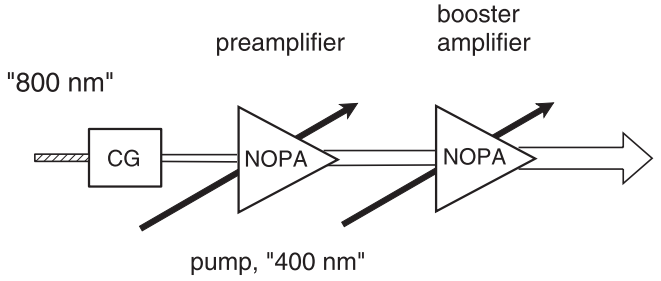

Fig. 5. Schematic of a two-stage blue-pumped NOPA for increased amplification and tunability

As indicated in Fig. 3, the continuum out of the sapphire plate contains spectral components out to 1600 nm. To enhance the NIR part of the continuum a somewhat higher pulse energy was used for the generation and the drastically different beam divergence had to be accounted for. With proper overall alignment a tuning range from 865 to 1600 nm was achieved with system 2. The output energies scaled from 7.5 μJ to 2.5 μJ with increasing wavelength. At the shorter wavelengths 20 fs duration was demonstrated with an increase to just below 50 fs at 1600 nm. Typical spectral distributions (after frequency-doubling in a 100 μm BBO crystal) and autocorrelation traces are shown in Fig. 6. The limited phase-matching bandwidth allows for nearly perfect Gaussian-shaped spectra and time–bandwidth products between 0.35 and 0.55.

As mentioned above, a blue-pumped NOPA might not be the prime choice for the generation of NIR pulses if a setup is designed from scratch. Our approach has, however, a number of practical advantages: 1) an existing blue-pumped NOPA can be used with minor modification of the alignment, 2) the 865 to 1100 nm spectral range can be accessed directly and quite conveniently. In a red-pumped OPA the idler has to be frequency-doubled to reach this range, 3) the noncollinear geometry allows the separation of the pump, signal and idler wavelengths purely by geometry without the need for any dichroic optics with their inherent phase problems, and 4) when operating the blue-pumped NOPA in the NIR, the off-axis beam generated simultaneously is visible and quite bright. It is therefore extremely useful in the alignment and there is no need for NIR viewers.

Another possibility to generate NIR pulses in a NOPA is type II phase matching in BBO. The e- polarized visible beam has a higher group velocity than the o-polarized NIR one and consequently an angle Ω for group-velocity matching can be found according to Sect. 2. The resulting pump/seed angle is fairly large for short-wavelength RGAs but becomes reasonable for longer pump wavelengths. We were able to operate a type II phase-matched NOPA pumped by system 3 and to produce pulses as short as 20 fs [30, 31]. This concept might be helpful in future developments utilizing differing nonlinear crystals and/or pump sources.

5 Operation around 800 nm with intermediate continuum generation

The spectrum of the seed continuum shown in Fig. 3 clearly displays a highly structured shape around the pump wavelength of 800 nm. This appearance is quite typical for self-phase modulation and the chirp has been found to increase dramatically in this region [24]. Attempts to generate ultrashort tunable pulses from this seed light were not very successful. At some wavelengths double pulses were found and in a range of ±10% from the RGA wavelength it was always difficult to suppress NOPA operation at the RGA fundamental. Only the generation of pulses with a length around 100 fs and far from an ideal time–bandwidth product was routinely possible.

Improved filtering carries the problem of phase distortions and a temporal manipulation to select a suitable portion of the seed light is difficult to implement in the 100 fs domain. Therefore we investigated the possibility to generate a more-suitable seed light by starting from pulses at an intermediate wavelength generated in a first NOPA stage. At first sight, visible pulses seem quite convenient to generate the continuum. However, practical problems with the necessary spectral filtering and the fairly high chirp of the visible pulses have not yet been overcome. On the contrary, operation of the first stage in the NIR has been found to be quite practical. The resulting setup is shown schematically in Fig. 7. The first continuum generator (CG) is pumped by the RGA fundamental and both amplifiers by the second harmonic.

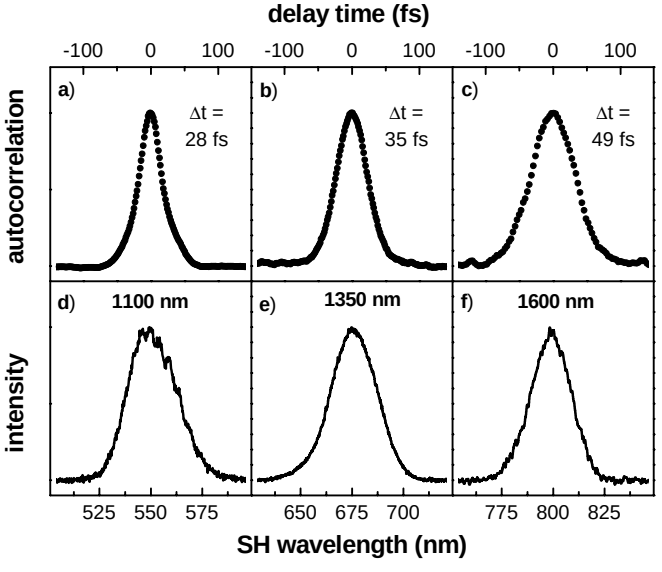

Fig. 6a–f. NIR pulses generated in a two-stage NOPA. **a–c** autocorrelation traces showing the sub-50-fs pulse lengths. **d–f** corresponding spectra. The pulses were frequency-doubled in a 100 μm BBO crystal and the resulting visible spectra recorded (see text)

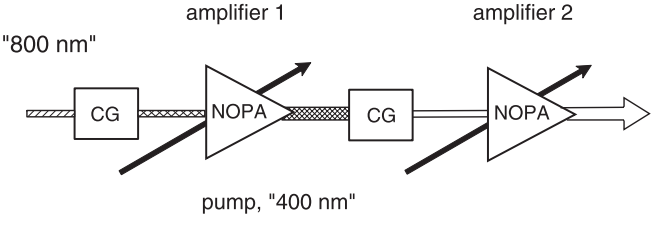

Fig. 7. Setup for the generation of tunable sub-50-fs pulses around 800 nm. The first continuum generator (CG) and amplifier are used to generate pulses around 1100 nm. They are also used to generate a second continuum. Parts of this continuum are finally amplified in the second amplifier

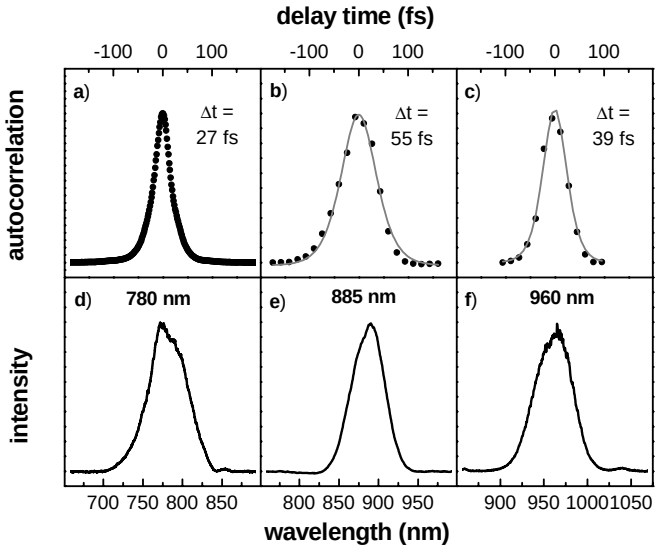

Fig. 8a–f. Characterization of various pulses generated with an intermediate continuum. **a–c** autocorrelation traces; **d–f** spectra

The additional continuum generator can easily be added into the two-stage setup already described for the generation of NIR pulses.

The characterization of pulses generated in a two-stage NOPA with intermediate continuum generator is shown in Fig. 8. Different RGA systems were used: the 775 nm pump system 2 for (a) and (d) and the 860 nm system 3 for (b), (c), (e) and (f). The production of these pulses will be described first.

Amplifier 1 was operated at 1200 nm and it produced about 3 μJ pulses after filtering the output with a Schott RG 1000 filter. This filter was employed to suppress traces of frequency-doubled output and to block the visible part of the seed light. In a similar fashion a dielectric filter was used to block the strong RGA fundamental contained in the seed light from reaching the amplifier 1. 1 μJ of the remaining 1200 nm pulse was then focused into a 2 mm sapphire plate with a 40-mm-focal-length achromatic lens. The resulting continuum was recollimated with a second identical lens and contained sufficient spectral components around the RGA wavelength.

A 2 mm BBO crystal cut for type II phase matching ($\theta = 55°, \varphi = 30°$) was used in the second amplifier. From 90 μJ of blue-pump light 6 μJ pulses at 960 nm and 4.5 μJ pulses at 885 nm were generated. The pulses were recompressed in a prism compressor composed of two SF10 prisms at a distance of about 45 cm. The autocorrelations were measured with a thin KDP SHG crystal and the spectra in a multichannel spectrometer. The spectral widths of 49 and 50 nm at 885 and 960 nm result in a time–bandwidth product about twice the Fourier limit.

For the generation of the 780 nm pulses from system 2 the first amplifier was operated at 1000 nm and we also used suitable filters for blocking unwanted wavelengths. A 2 mm type I BBO was used in amplifier 2 resulting in 3 μJ output with a spectral width of 57 nm and a time–bandwidth product of 0.7.

In summary, we find that even in the problematic range around the RGA fundamental fully tunable pulses with sub-50-fs length can be generated from a blue-pumped NOPA if a two-stage setup with an intermediate continuum generator is used. Improvements in the generation of clean and compressible white-light continua around the pump wavelength should further simplify the setup.

6 Two-color spectrometer with sub-30-fs cross-correlation

For many spectroscopic applications two independently tunable and fully synchronized sources of extremely short pulses are needed to supply the pump and probe pulses. Since a NOPA can well be pumped by 200 μJ of RGA fundamental, the typical output energies from commercial RGAs of above 1 mJ allow the parallel operation of two or more NOPAs. In our laboratories such two-color setups are routinely used and we find no detectable jitter between the two NOPAs. SHG cross- correlation curves with a width well below 30 fs are observed at the position of the spectroscopic sample [30].

The measurement of the cross-correlation for such short and broadband pulses is far from trivial. If a 100 μm BBO crystal is used, suitably balanced chirps on the two pulses can result in unrealistically low correlation widths. Only with crystals as thin as 25 μm or in appropriate photodiodes have we been able to measure the correct cross-correlation. These investigations will be reported in a separate publication.

The total signal fluctuations in a pump–probe experiment can be kept as low as 1%–2% with proper alignment of the RGA and the NOPAs. This very low value renders a high sensitivity to the pump–probe spectrometer. We routinely observe transient absorption changes of less than 10^{-4} for averaging over only a few hundred pulses.

A first investigation of the ultrafast S_1 decay of azulene molecules in solution has already been published [46]. We excited the molecules with wavelengths between 520 and 720 nm and were able to show that the nonradiative decay depends strongly on the excess vibrational energy deposited in the electronically excited state. In addition, the high temporal resolution allowed for the first time the observation of vibrational wavepackets in azulene.

A comprehensive investigation of the excited-state intramolecular proton transfer in 2-(2′-hydroxyphenyl)benzothiazole was performed with 347 nm excitation pulses generated by frequency doubling the output of one NOPA and tuning the probe pulses between 450 and 680 nm. At all wavelengths strong oscillatory contributions to the observed signal due to chelat ring vibrations were found, with vibrational frequencies as high as 500 cm^{-1} clearly resolved [47].

A first report on the ultrafast photoinduced electron transfer in coumarin 343-sensitized TiO_2 colloidal solutions employing a tunable visible probe pulse from a NOPA has just appeared [48]. Many more such investigations of research in natural or synthetic photosynthesis and photocells will greatly benefit from the drastically improved possibilities in pulse generation.

Finally, we want to mention an outstanding demonstration of the capabilities of NOPAs reported by Cerullo et al. [49]. They investigated the real-time vibronic coupling dynamics in conjugated oligomers and were able to resolve phonon modes up to 1454 cm^{-1}. This shows that real-time

vibrational spectroscopy at freely chosen excitation wavelengths can now observe all but the very highest vibrations in molecules.

7 Summary

The recently developed technique of noncollinear phase matching in blue-pumped optical parametric amplifiers for extremely broadband amplification has matured to the point where NOPAs can now provide fully tunable pulses from 460 to 1600 nm. The accessible ranges are summarized together with the typical pulse lengths in Fig. 3. In the visible, tuning from 460 to 700 nm is given by the continuum used to seed the NOPA. The equivalence between the broad amplification bandwidth needed to support sub-20-fs pulses and the effective group-velocity matching of signal and idler pulses is well understood. In the NIR the NOPA is still a very useful tool even though this principle is no longer applicable. For the first time we have reported the use of an intermediate continuum that allows the generation of extremely short pulses even close to the degeneracy point, i.e. at the RGA fundamental.

In Fig. 9 we show an overview of pulse lengths and pulse energies that were collected from various setups in our laboratories as spectroscopic experiments were performed. The energy is largest for the shortest wavelengths and decreases more or less monotonically with increasing wavelength. This is due to the fact that a given number of photons amounts to decreasing energy with increasing wavelength. As a rule of thumb the quantum-conversion efficiency in a NOPA is found to be 15%. The pulse lengths are around and below 20 fs in the visible and increase up to 50 fs at 1600 nm. All these lengths represent a dramatic shortening from the typical 100 fs pump pulses utilized. We actually find that very short pump pulses are of no advantage for the generation of tunable visible pulses.

The principle of noncollinear phase matching and effective group-velocity matching is certainly not restricted to BBO crystals and Ti:sapphire regenerative amplifiers. It will be interesting to see how other spectral ranges like the UV and the mid IR can profit from the new possibilities. Certainly ultrafast spectroscopy in physics, chemistry and biology will greatly benefit from the newly available chances.

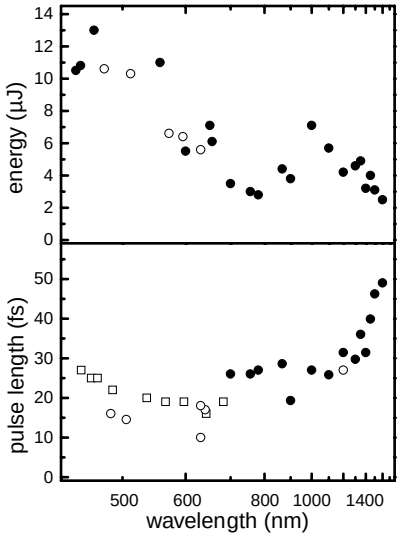

Fig. 9. Summary of the output energies and pulse lengths used in various spectroscopic experiments. The different symbols correspond to different regenerative amplifiers and NOPA implementations

Acknowledgements. We thank Dr. Thomas Wilhelm for important work in the early stages of the developments and Dilor GmbH/Clark-MXR Inc. for the generous loan of the CPA-2001 femtosecond amplifier used in some of the experiments. Financial support from the Deutsche Forschungsgemeinschaft and the Fonds der Chemischen Industrie is gratefully acknowledged.

Note added in proof

Recently we have increased the output of the two-stage NOPA to 20 μJ and extended the tuning range to 1–7 μm.

References

1. R.L. Fork, B.I. Greene, C.V. Shank: Appl. Phys. Lett. **38**, 671 (1981)
2. R.L. Fork, C.V. Shank, R.T. Yen: Appl. Phys. Lett. **41**, 223 (1982)
3. R.W. Schoenlein, J.-Y. Bigot, M.T. Portella, C.V. Shank: Appl. Phys. Lett. **58**, 801 (1991)
4. R.L. Fork, C.H. Brito Cruz, P.C. Becker, C.V. Shank: Opt. Lett. **12**, 483 (1987)
5. J. Squier, F. Salin, G. Mourou, D. Harter: Opt. Lett. **16**, 324 (1991)
6. V. Petrov, F. Seifert, F. Noack: Appl. Phys. Lett. **65**, 268 (1994)
7. M. Nisoli, S. De Silvestri, V. Magni, O. Svelto, R. Danielius, A. Piskarskas, G. Valiulis, A. Varanavicius: Opt. Lett. **19**, 1973 (1994)
8. V.V. Yakovlev, B. Kohler, K.R. Wilson: Opt. Lett. **19**, 2000 (1994)
9. R. Danielius, A. Piskarskas, P. Di Trapani, A. Andreoni, C. Solcia, P. Foggi: Appl. Opt. **35**, 5336 (1996)
10. M. Sueptitz, R.A. Kaindl, S. Lutgen, M. Woerner, E. Riedle: Opt. Commun. **131**, 195 (1996)
11. K.R. Wilson, V.V. Yakovlev: J. Opt. Soc. Am. B **14**, 444 (1997)
12. V. Petrov, F. Seifert, F. Noack: Appl. Opt. **33**, 6988 (1994)
13. V. Petrov, F. Seifert, O. Kittelmann, J. Ringling, F. Noack: J. Appl. Phys. **76**, 7704 (1994)
14. S.R. Greenfield, M.R. Wasielewski: Appl. Opt. **34**, 2688 (1995)
15. P. Di Trapani, A. Andreoni, P. Foggi, C. Solcia, R. Danielius, A. Piskarskas: Opt. Commun. **119**, 327 (1995)
16. P. Di Trapani, A. Andreoni, C. Solcia, G.P. Banfi, R. Danielius, A. Piskarskas, P. Foggi: J. Opt. Soc. Am. B. **14**, 1245 (1997)
17. M.K. Reed, M.K. Steiner-Shepard, D.K. Negus: Opt. Lett. **19**, 1855 (1994)
18. M.K. Reed, M.K. Steiner-Shepard, M.S. Armas, D.K. Negus: J. Opt. Soc. Am. B **12**, 2229 (1995)
19. T.J. Driscoll, G.M. Gale, F. Hache: Opt. Commun. **110**, 638 (1994)
20. G.M. Gale, M. Cavallari, T.J. Driscoll, F. Hache: Opt. Lett. **20**, 1562 (1995)
21. G.M. Gale, M. Cavallari, F. Hache: J. Opt. Soc. Am. B **15**, 702 (1998)
22. T. Wilhelm, J. Piel, E. Riedle: Opt. Lett. **22**, 1494 (1997)
23. T. Wilhelm, E. Riedle: Opt. Phot. News **12**, 50 (1997)
24. G. Cerullo, M. Nisoli, S. De Silvestri: Appl. Phys. Lett. **71**, 3616 (1997)
25. G. Cerullo, M. Nisoli, S. Stagira, S. De Silvestri: Opt. Lett. **23**, 1283 (1998)
26. G. Cerullo, M. Nisoli, S. Stagira, S. De Silvestri, G. Tempea, F. Krausz, K. Ferencz: Opt. Lett. **24**, 1529 (1999)
27. A. Shirakawa, T. Kobayashi: Appl. Phys. Lett. **72**, 147 (1998)
28. A. Shirakawa, I. Sakane, T. Kobayashi: Opt. Lett. **23**, 1292 (1998)
29. A. Shirakawa, I. Sakane, M. Takasaka, T. Kobayashi: Appl. Phys. Lett. **74**, 2268 (1999)
30. S. Lochbrunner, T. Wilhelm, J. Piel, P. Huppmann, S. Spörlein, E. Riedle: *Ultrafast Phenomena XI*, ed. by T. Elsaesser, J.G. Fujimoto, D.A. Wiersma, W. Zinth (Springer, Berlin 1998) p. 57
31. S. Lochbrunner, T. Wilhelm, J. Piel, S. Spörlein, E. Riedle: *OSA Trends in Optics and Photonics*, Vol. 26, *Advanced Solid-State Lasers*, ed.

by M.M. Fejer, H. Injeyan, U. Keller (OSA, Washington, DC 1999) p. 366
32. J. Piel, M. Beutter, E. Riedle: Opt. Lett. **25**, 180 (2000)
33. S. Reisner, M. Gutmann: J. Opt. Soc. Am. B **16**, 1801 (1999)
34. SNLO nonlinear optics code available from A.V. Smith, Sandia National Laboratories, Albuquerque, NM 87185-1423
35. M.K. Reed, M.S. Armas, M.K. Steiner-Shepard, D.K. Negus: Opt. Lett. **20**, 605 (1995)
36. A. Brodeur, S.L. Chin: J. Opt. Soc. Am. B **16**, 637 (1999)
37. M. Nisoli, S. Stagira, S. De Silvestri, O. Svelto, G. Valiulis, A. Varanavicius: Opt. Lett. **23**, 630 (1998)
38. S. Fournier, R. López-Martens, C. Le Blanc, E. Baubeau, F. Salin: Opt. Lett. **23**, 627 (1998)
39. R. López-Martens, S. Fournier, C. Le Blanc, E. Baubeau, F. Salin: IEEE J. Sel. Top. Quantum Electron. **4**, 230 (1998)
40. A. Andreoni, M. Bondani: Appl. Opt. **37**, 2414 (1998)
41. J. Zhang, Z. Xu, Y. Kong, C. Yu, Y. Wu: Appl. Opt. **37**, 3299 (1998)
42. I.N. Ross, P. Matousek, M. Towrie, A.J. Langley, J.L. Collier: Opt. Commun. **144**, 125 (1997)
43. A. Dubietis, G. Jonušauskas, A. Piskarskas: Opt. Commun. **88**, 437 (1992)
44. V. Krylov, O. Ollikainen, J. Gallus, U. Wild, A. Rebane, A. Kalintsev: Opt. Lett. **23**, 100 (1998)
45. D. Zeidler, T. Hornung, P. Proch, M. Motzkus: Appl. Phys. B, in print
46. A.J. Wurzer, T. Wilhelm, J. Piel, E. Riedle: Chem. Phys. Lett. **299**, 296 (1999)
47. A.J. Wurzer, S. Lochbrunner, E. Riedle: Appl. Phys. B, this issue
48. J. Wachtveitl, R. Huber, S. Spörlein, J.E. Moser, M. Grätzel: Int. J. Photoenergy **1**, 1 (1999)
49. G. Cerullo, G. Lanzani, M. Muccini, C. Taliani, S. De Silvestri: Phys. Rev. Lett. **83**, 231 (1999)